Supporting Information

Miller et al. 10.1073/pnas.0913697107

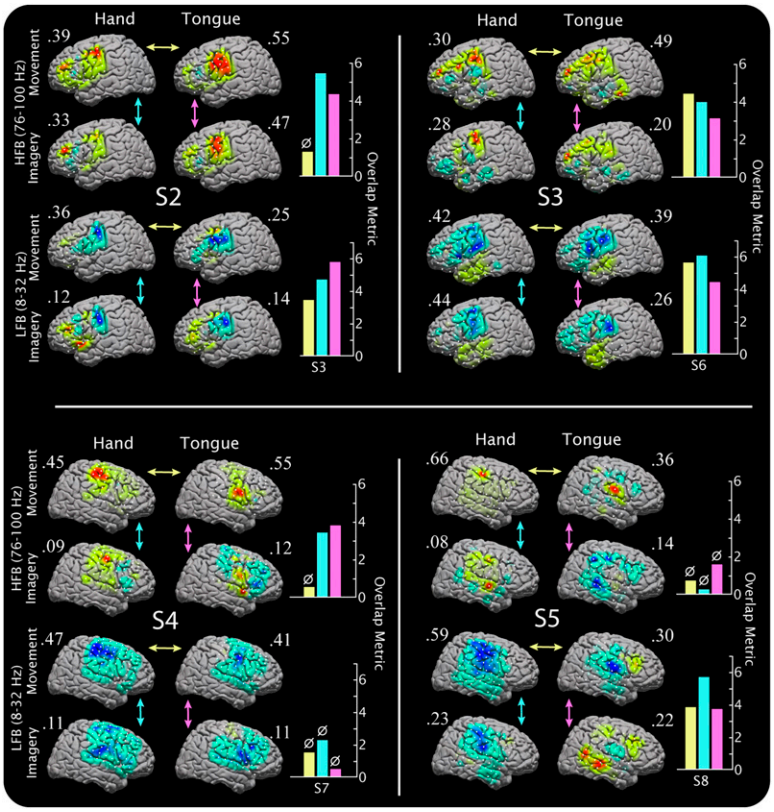

Fig. S1. Spectral changes in cortical surface potentials during paired hand and tongue movement and imagery for subjects 2–5 (denoted S# in middle of brain plots). This is the same as Fig. 1 *C* and *D*, for additional subjects. In each map, the activation (HFB, top two rows in each quadrant; LFB, bottom two rows, activation calculation described in Fig. S10) is scaled to the maximum absolute activation (value indicated in the upper left corner of each map) and plotted to a template cortex. The overlap between maps is quantified according to the bootstrapped overlapping method described in Fig. S3. This overlap is shown on the adjacent bars, where yellow denotes hand–tongue overlap for movement, light blue denotes hand movement–imagery overlap, and pink denotes tongue movement–imagery overlap (corresponding to arrows). The circle-slash indicates a $P > 0.01$ significance associated with the overlap (i.e., a >1% chance that the overlap seen is due to chance).

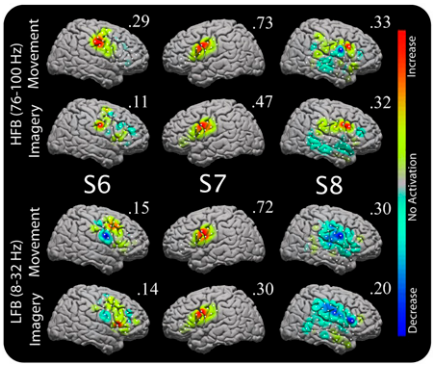

Fig. S2. Actual and imagined tongue movement activations for subjects 6–8 (HFB, top two rows; LFB, bottom two rows), plotted (as in Fig. 1 and Fig. S1, but no hand movement/imagery task was performed). The HFB overlap metric (significance) for subjects 6/7/8 was 2.20 ($P = 0.03$)/1.96 ($P = 0.04$)/3.73 ($P = 2 \times 10^{-4}$). The LFB overlap metric (significance) for subjects 6/7/8 was 3.59 ($P = 8 \times 10^{-5}$)/1.16 ($P = 0.10$)/2.17 ($P = 0.02$).

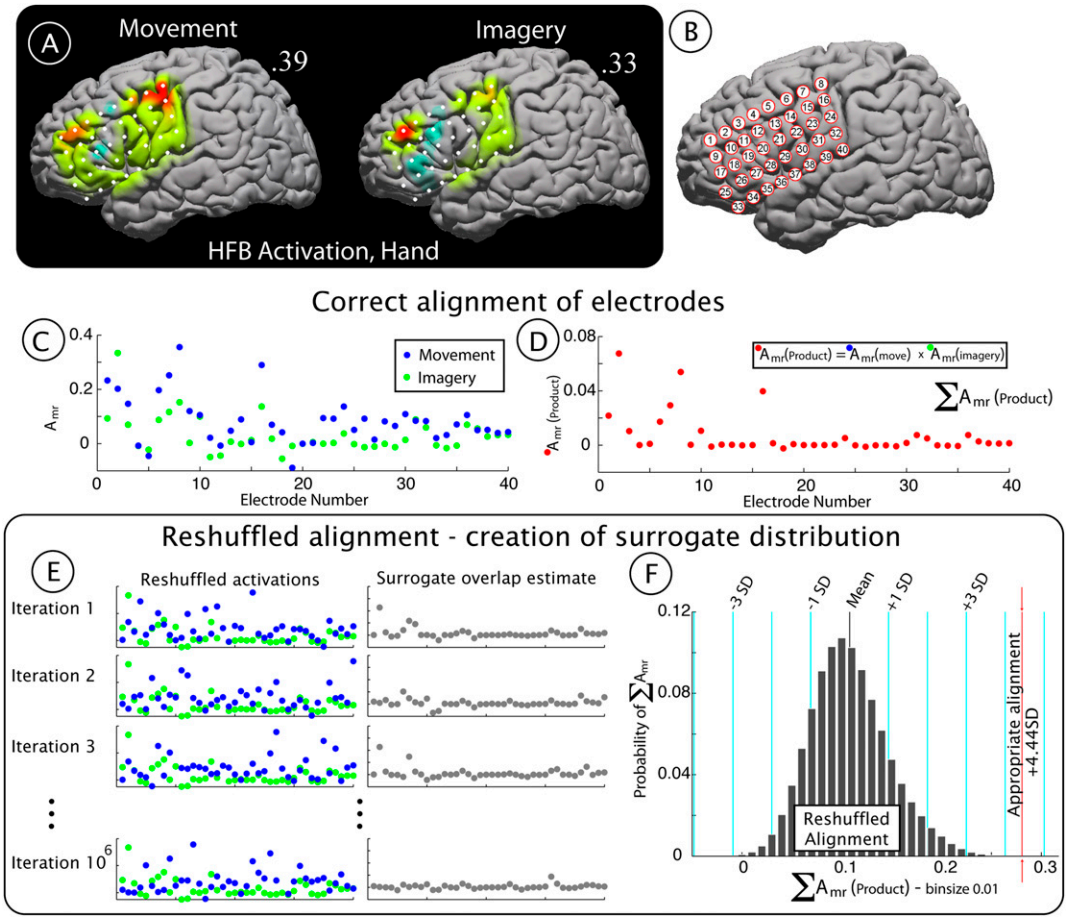

Fig. S3. Method for quantifying overlap in spatial distribution. (*A*) We would like to quantify the overlap between two patterns of activation, one for actual movement, and one for imagery. Subject 2 is shown for illustration, during hand movement and imagery. (*B*) To do this, we assess the activity at each electrode (numbering on brain plot indicates electrode number). (*C*) The activity at each electrode is quantified independently using the approach illustrated in Fig. S10. (*D*) The overlap can be quantified by taking the dot product across electrodes (in this way, the activities are paired together at each electrode). (*E*) Given a similar distribution of activation values, we can probe all of the possible conformations that they might have taken, by reshuffling the electrode positions for one of the cases (movement), and recalculating the dot product. This is done 10^6 times, and a distribution of surrogate dot products is generated. (*F*) We can use this surrogate distribution to estimate a *P* value for the significance of the overlap (in this example, $P = 2 \times 10^{-6}$). The distribution of surrogate values tends to be approximately Gaussian (in this case, kurtosis = 3.15). Because of this, the value of our actual overlap, in *z*-score units (of the surrogate distribution; here, 4.44), can be used as a quantitative measure of overlap.

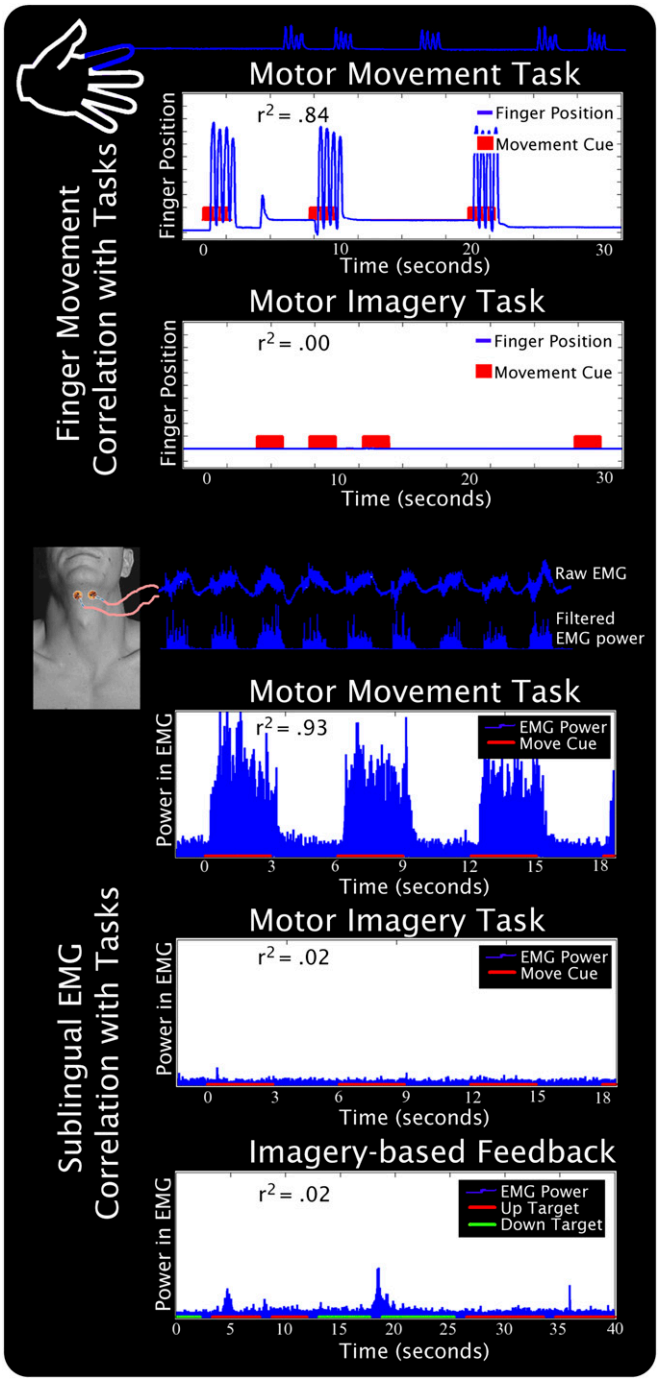

Fig. S4. Verifying imagery. Where possible, subjects wore a dataglove (5DT, Irvine, CA) or were monitored using clinical EMG sensors to verify that movement was absent during imagery. Subject 1 wore the dataglove, which recorded index finger position during the interval-based finger movement task. During the motor movement task, the squared correlation of index finger position with the cue (movement vs. rest) was significant ($r^2 = 0.84$, $P < 0.001$). There was no significant correlation of finger position with cue during the hand motor imagery task (second panel). Subject 8 had a sublingual differential EMG pair in place during a tongue motor task, a tongue motor imagery task, and an imagery based feedback task. The EMG signal was band-stop-filtered from 57 to 63 Hz, 117 to 123 Hz, and 177 to 183 Hz to reject line noise (third-order Butterworth digital filter, forward and backward to eliminate phase distortion). It was then high-pass-filtered at 20 Hz noise (third-order Butterworth digital filter, forward and backward) and squared to obtain the "filtered EMG power." The power in the EMG was significantly correlated with the tongue motor movement task (cross-correlation $r^2 = 0.93$, $P < 0.001$) but was not correlated with either the tongue imagery or imagery-based feedback task.

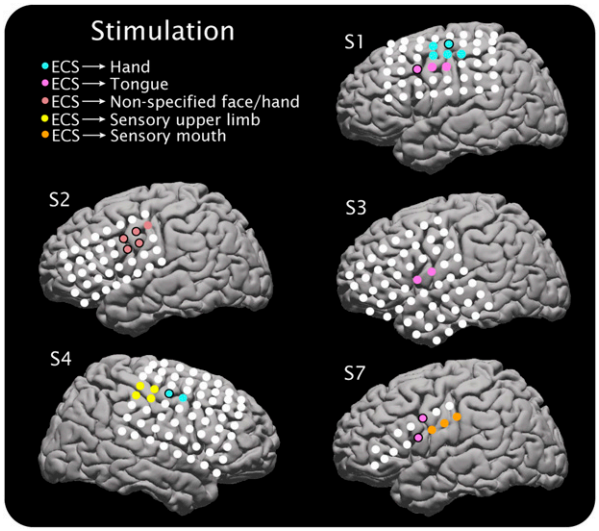

Fig. S5. Functional localization of primary motor areas by electrocortical stimulation (ECS), in five subjects (denoted S#). For clinical reasons, it was performed for these 5 subjects, and not the other 3. Language and nonrelevant functionally identified sites are not shown. For subjects 1, 2, 4, and 7, imagery of a type of movement produced significant HFB change ($P > 0.05$) at a site where ECS induced movement of that type, as shown with circled black electrodes (see Fig. 1 and Fig. S1). In the case of subject 3, imagery produced significant HFB change only at a frontal site, and not at the site that induced motor movement (motor movement also produced HFB change at that frontal site, but not at the ECS site). Electrocortical stimulation (ECS) to create transient lesions or induce overt movements, extra- or intraoperatively, is the established method to clinically localize function in the brain (1–3). This process of stimulation is critical to minimizing risk in neurological surgeries that involve resection of seizure focus, tumor, or vascular malformation (4–6), and predicts functional outcome (6, 7). Effective mapping requires that all electrodes be stimulated with varying amounts of amperage and requires ongoing and consistent patient participation. Stimulation often leads after discharges that can induce seizures or provide misleading functional responses from distally stimulated cortex. The stimulation mapping process in the context of subdural electrode arrays is often incomplete either because it is prematurely aborted by an induced seizure, or stopped once an acceptable surgical margin is obtained. The entire array is rarely surveyed. For these reasons, many of the activation maps in this study are devoid of stimulation locations or contain incomplete stimulation information. In this sense, there are only positive stimulation results, without negative control. The meaningful question in the context of this study is whether motor imagery produces neuronal population activity, revealed by changes in the HFB, in primary motor areas (i.e., Brodmann areas 4 and 6) that are identified by ECS. As shown in this study by subjects 1, 2, 4, and 7, imagery does result in cortical activity in primary motor areas.

1. Ojemann G, Ojemann J, Lettich E, Berger M (1989) Cortical language localization in left, dominant hemisphere. An electrical stimulation mapping investigation in 117 patients. *J Neurosurg* 71:316–326.
2. Chitoku S, et al. (2001) Extraoperative cortical stimulation of motor function in children. *Pediatr Neurol* 24:344–350.
3. Branco DM, et al. (2003) Functional variability of the human cortical motor map: electrical stimulation findings in perirolandic epilepsy surgery. *J Clin Neurophysiol* 20:17–25.
4. Berger MS, Kincaid J, Ojemann GA, Lettich E (1989) Brain mapping techniques to maximize resection, safety, and seizure control in children with brain tumors. *Neurosurgery* 25: 786–792.
5. Burchiel KJ, Clarke H, Ojemann GA, Dacey RG, Winn HR (1989) Use of stimulation mapping and corticography in the excision of arteriovenous malformations in sensorimotor and language-related neocortex. *Neurosurgery* 24:322–327.
6. Haglund MM, Berger MS, Shamseldin M, Lettich E, Ojemann GA (1994) Cortical localization of temporal lobe language sites in patients with gliomas. *Neurosurgery* 34:567–576, discussion 576.
7. Keles GE, et al. (2004) Intraoperative subcortical stimulation mapping for hemispherical perirolandic gliomas located within or adjacent to the descending motor pathways: evaluation of morbidity and assessment of functional outcome in 294 patients. *J Neurosurg* 100:369–375.

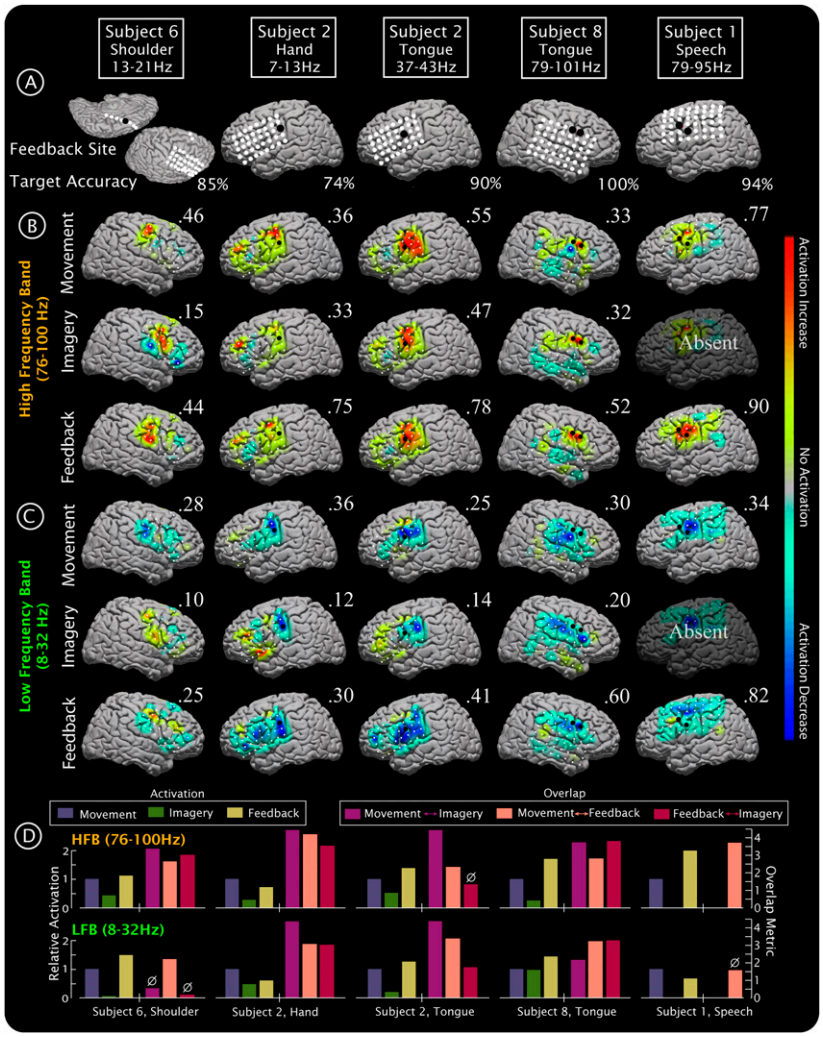

Fig. S6. Augmentation of cortical activity during learning. (*A*) Site of feedback, shown with a black dot, and electrode positions for subjects 6, 2, 8, and 1. The box above each template brain indicates the subject, the paired motor/imagery/feedback modality, and the frequency range used for feedback. The feedback accuracy is the percentage of time the subject was able to hit the correct target using this feedback feature. "Speech" for subject 1 was repetition of the word "move." (*B*) HFB (76–100 Hz) ECoG-based brain activation maps for actual movement, imagined movement, and feedback-based BCI cursor control. Activation in each map is scaled to the maximum activation (absolute-value, noted by the number above each template brain). Subject 1 did not perform a speech (word repetition) imagery task. (*C*) As in *B*, for the LFB (8–32 Hz). (*D*) The relative activation (also shown in Fig. 4) during each of the three conditions is shown for the HFB (*Upper*) and LFB (*Lower*) on the left side of each set of axes, for each subject. Relative activation was computed by dividing the imagery- and feedback-related activation by the activation for actual movement, and normalizing the magnitude of activation for actual movement to 1 for all plots. The bar plots show that in most cases, the magnitude of feedback-related activation after learning exceeds the magnitude of activation for actual movement. The overlap between each of the conditions is shown with the purple/pink/magenta bars, for the HFB (*Upper*) and LFB (*Lower*) on the right side of each set of axes, for each subject.

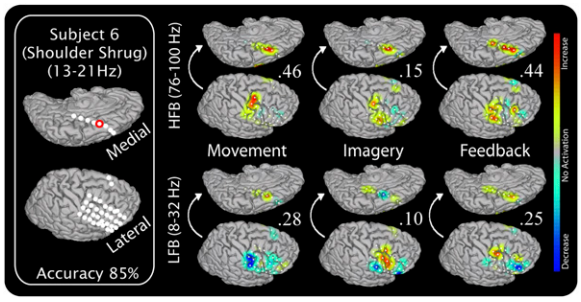

Fig. S7. Spectral changes in ECoG following shoulder imagery feedback for subject S6 (feedback from 13 to 21 Hz) on a medial electrode (red circle; same as in Fig. S6 *A*–*C*).

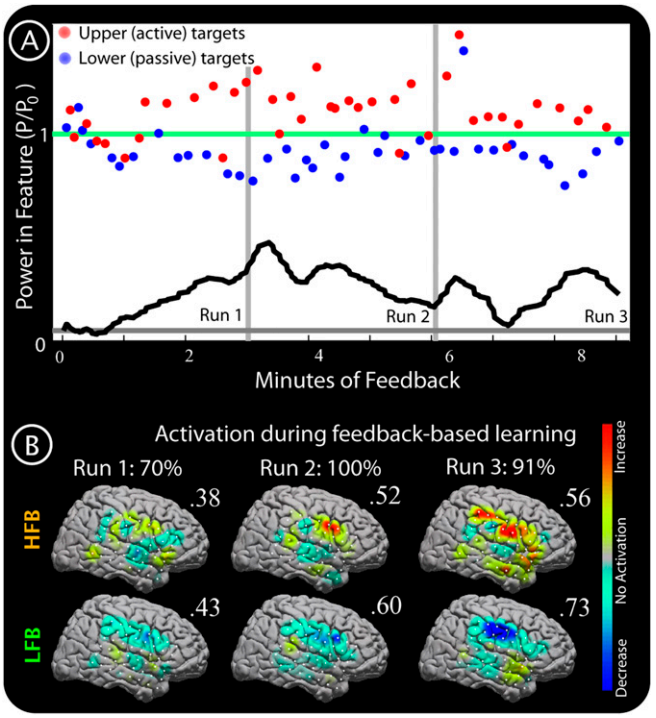

Fig. S8. Changes in cortical activity during brain–computer interface control for subject 8 during tongue motor imagery (details as in Fig. 5). Three consecutive runs with feedback are shown. The subject reported being disinterested in the last run.

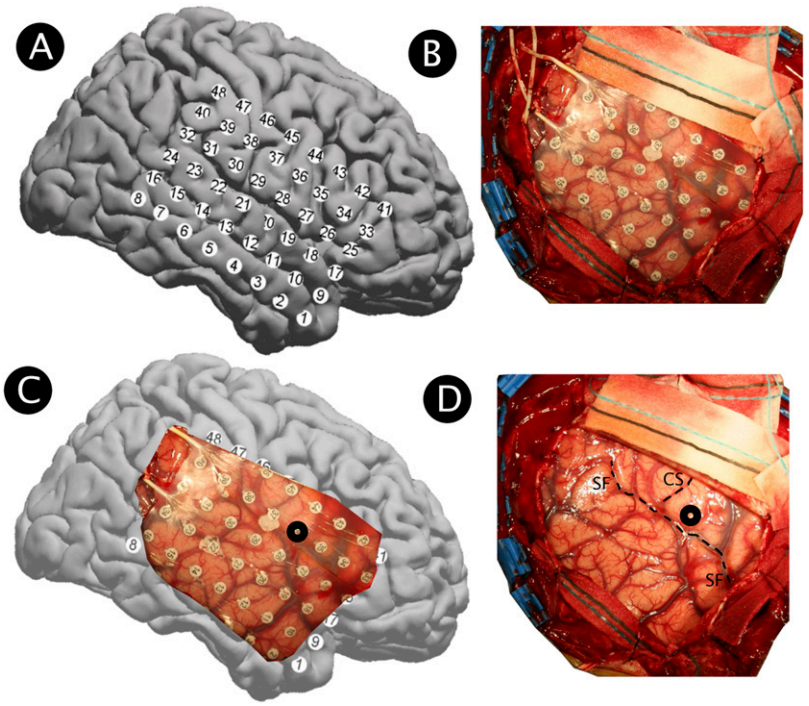

Fig. S9. Coregistration of electrodes, comparing anatomical photographs, subject 8. (*A*) Electrode positions interpolated from x-ray (on the AFNI template) estimated with the LOC package. (*B*) Electrode positions shown from an intraoperative picture. (*C*) The aperture in *B* projected onto *C*, with the feedback electrode shown with a black circle. (*D*) The location of the electrode on the exposed brain (intraoperative picture). SF, Sylvian fissure; CS, central sulcus.

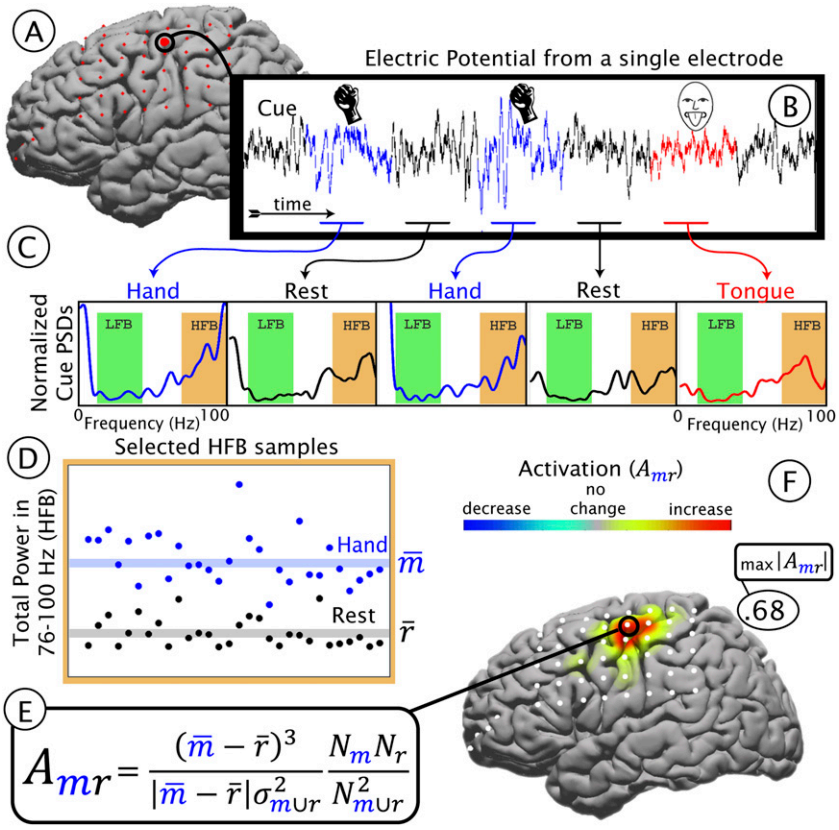

Fig. S10. Method for calculating and displaying activation. (*A*) An electrode from primary motor cortex from subject 1 shown for illustration. (*B*) A subject performed an interval-based motor movement or kinesthetic imagery [Neuper C, et al. (2005) *Brain Res Cogn Brain Res* 25:668–677] task. The raw signal (re-referenced with respect to the common average) from each electrode is divided into 3-s epochs based on the stimulus to move (or to imagine moving) the hand or tongue, and resting. A subset of each epoch, the time corresponding to 0.5–2 s into that epoch (shown in the horizontal lines below the raw data), is selected for analysis, to account for behavioral lag. (*C*) The power spectral density of each epoch was calculated every 1 Hz using a fast Fourier transform with 0.25-s Hann-windowed segments, stepping with an overlap of 0.1 s (Welch's averaged periodogram method). Each power spectrum is then normalized by dividing the power at each frequency bin by the average power at that frequency bin, taken across all epochs. (*D*) Total power in a low-frequency band (LFB) (8–32 Hz) and a high-frequency band (HFB) (76–100 Hz) is calculated for each epoch of each type. The plot shows samples of HFB power during hand movement and rest. (*E*) The activation, A_{mr}, is calculated for each movement or imagery modality. In the case of a mixed modality experimental run, the distribution of samples of power for each modality are compared only with the samples of power for rest epochs that followed epochs of that kind (i.e., hand movement epochs are compared with rest epochs that followed hand movement, and not those that followed tongue movement). Activation was quantified as the signed square of the cross-correlation to reflect an increase or a decrease in the band-limited PSD for movement (m) with respect to rest (r) (or, in the case of a target task, whether one target represents an increase or decrease in power with respect to the other target). This metric indicates how much of the variation in the joint data set $\sigma^2_{m \cup r}$ can be accounted for by the fact that subdistributions *m* and *r* might have different means, $\bar{m}$ and $\bar{r}$ (N_m and N_r are the number of samples of type *m* and *r*, respectively, and $N_{m \cup r} = N_m + N_r$). (*F*) The activation obtained for each electrode is used to scale a spherical Gaussian kernel (σ = 5 mm) centered at the Talairach location obtained for that electrode using the LOC package [Miller KJ, et al. (2007) *J Neurosci Methods* 162:303–308], and all kernels are linearly superimposed to obtain a cortical map. The activation is scaled to the maximum absolute activation (indicated to the upper left of the map), with the color scale shown (dark red, maximum increase in activation; dark blue, maximum decrease in activation; gray, no activation). These maps are generated for each subject, each band (HFB or LFB), and each movement or imagery modality.

Table S1. Patient descriptions and characteristics

Patient	Age	Sex	Hand	Grid location	Seizure focus
1	18	F	R	L Frontal	L Frontal
2	23	M	R	L Frontotemporal	L Temporal
3	41	M	L	L Frontotemporal	L Temporal
4	38	M	R	R Frontal	R Frontal
5	48	M`	R	R Temporal-parietal-occipital	R Temporal-occipital
6	31	F	R	R Frontotemporal	R Insula
7	12	M	R	L Frontotemporal	R Temporal
8	32	M	R	R Frontotemporal	L Temporal